Eur. Phys. J. B **38**, 571–580 (2004)
DOI: 10.1140/epjb/e2004-00154-5

THE EUROPEAN PHYSICAL JOURNAL B

# Field induced magnetic ordering transition in Kondo insulators

I. Milat[1,a], F. Assaad[1,2], and M. Sigrist[1]

[1] Theoretische Physik, ETH-Hönggerberg, 8093 Zürich, Switzerland
[2] Universität Würzburg, Am Hubland, 97074 Würzburg, Germany

Received 17 December 2003
Published online 8 June 2004 – 

**Abstract.** We study the 2D Kondo insulators in a uniform magnetic field using quantum Monte Carlo simulations of the particle-hole symmetric Kondo lattice model and a mean field analysis of the Periodic Anderson model. We find that the field induces a transition to an insulating, antiferromagnetically ordered phase with staggered moment in the plane perpendicular to the field. For fields in excess of the quasi-particle gap, corresponding to a metal in a simple band picture of the periodic Anderson model, we find that the metallic phase is unstable towards the spin density wave type ordering for any finite value of the interaction strength. This can be understood as a consequence of the perfect nesting of the particle and hole Fermi surfaces that emerge as the field closes the gap. We propose a phase diagram and investigate the quasi-particle and charge excitations in the magnetic field. We find good agreement between the mean-field and quantum Monte Carlo results.

**PACS.** 71.27.+a Strongly correlated electron systems; heavy fermions – 71.10.Fd Lattice fermion models (Hubbard model, etc.) – 71.30.+h Metal-insulator transitions and other electronic transitions – 75.30.Mb Valence fluctuation, Kondo lattice, and heavy-fermion phenomena – 75.30.Fv Spin-density waves

## 1 Introduction

Kondo insulators, or heavy fermion semiconductors, are materials containing at least one atom per formula unit with a partially filled $f$ or $d$ shell and exhibiting properties similar to very narrow gap semiconductors. CeRhAs, CeRhSb, $YB_{12}$, $Ce_3Bi_4Pt_3$ and $SmB_6$ are the most thoroughly investigated examples [1]. In the canonical model, the formation of the gap in Kondo insulators is a consequence of the hybridization between the conduction band and the effective $f$-electron level which gives rise to quasi-particle and spin-gaps at low temperatures. Adopting a band picture one can close the gap by applying a high magnetic field, since the gap is on the meV scale. Although experiments on $YB_{12}$ [2], $SmB_6$ [3] and $Ce_3Bi_4Pt_3$ [4] seem to support this simple picture, the exact nature of the field induced insulator to metal transition as well as the role played by the strong correlations remains far from understood.

Magnetic instabilities of the periodic Anderson model at half-filling have been studied extensively by slave boson mean field approximations [15,13,14]. A phase diagram as a function of the interaction strength was established and some thermodynamic and transport properties have been calculated. In these studies, the only effect of the magnetic field is assumed to be the stabilization of the ferromagnetically ordered state with respect to other magnetic configurations.

Carruzzo and Yu [10] studied the one dimensional, half-filled Kondo lattice in magnetic field using DMRG and bosonisation techniques. They found that although the spin gap closed at the critical field, the charge gap remained due to umklapp scattering They conclude that the 1D half-filled Kondo lattice is insulating at all fields.

The effect of the field in disordered Kondo insulators was treated by CPA in references [6,5]. The authors find that, in the absence of magnetic ordering, the magnetic field induces the insulator to metal transition in the universality class of density driven metal-insulator transitions. Based on scaling arguments the field dependence of the quasi-particle gap as well as the critical field as a function of temperature and impurity concentration were derived.

In this paper we present a detailed study of the field induced quantum phase transition in 2D particle-hole symmetric models of Kondo insulators. We present a mean field calculation appropriate for the small-$U$ limit of the periodic Anderson model. We find that the magnetic field induces a phase transition from the paramagnetic insulator into a canted antiferromagnetic insulator which remains stable at all field strengths (until all the electrons in the system align with the field). While zero-energy spin modes exist, we find that the field does not close the quasi-particle gap, if the lattice is bipartite, so that the metallic

[a] e-mail: igor.milat@ethz.ch

ground state is never induced by the field. We investigate more carefully the large-field limit using two effective models and reach essentially the same conclusion — on the bipartite lattice, the interaction is a relevant perturbation and the ground state remains insulating at all fields. The approximate treatments are complemented by a quantum Monte Carlo study of the particle hole symmetric Kondo lattice model in 2D. We find good agreement between the results.

Recently, Beach and collaborators studied the effect of the magnetic field on the Kondo insulators using a large-$N$ type mean field analysis of the Kondo lattice model and quantum Monte Carlo simulations [11]. They find that a large enough magnetic field induces a phase transition to a metallic ground state from the insulating canted antiferromagnetic state. The phase transition into the metallic state occurs when the $f$ moments decouple from the conduction band, i.e. the hybridization mean field vanishes at a certain critical field. The question naturally arises whether this phase transition is real or possibly an artifact of the large-$N$ mean field approach. Here we will show results which lead to a different conclusion: the insulating state induced by the magnetic field remains stable up to the full polarization of all electrons in the system, if the system is completely particle-hole symmetric. Thus the particle-hole symmetric Kondo insulator is an insulator at all fields.

The paper is organized as follows: in the next section we introduce the models used to describe Kondo insulators. In Section 3 the phase diagram in the presence of the magnetic field is obtained using a mean field approximation for the half-filled periodic Anderson model. In Section 4 we present a discussion of the Kondo lattice model in high magnetic fields. In Section 5 the results of the Quantum Monte Carlo simulations are presented and compared with the mean field calculations. We summarize our results in Section 6 and briefly comment on their relevance for the experimental systems.

## 2 Models

The canonical model used to describe the physics of the Kondo insulators is the periodic Anderson model (PAM) [1]. The PAM Hamiltonian, including the uniform magnetic field in the $z$-direction is

$$H_{PAM} = -\sum_{\langle i,j\rangle,\sigma} t_{ij} c^\dagger_{i\sigma} c_{j\sigma} + \epsilon_f \sum_{i\sigma} f^\dagger_{i\sigma} f_{i\sigma} + U \sum_i n^f_{i\uparrow} n^f_{i\downarrow} + \sum_{k,\sigma} (V f^\dagger_{k\sigma} c_{k\sigma} + \text{H.c.}) - g\mu_B \vec{B} \cdot \sum_i (\vec{S}^f_i + \vec{S}^c_i). \quad (1)$$

Here all the symbols have their usual meaning. The PAM describes a two band system in which one band (conduction electron, $c$ band) is dispersive and uncorrelated and the other ($f$ band) dispersionless and strongly correlated. $t_{ij}$ is the hopping matrix element in the $c$ band and $U$ the local Coulomb interaction in the $f$ band. The two bands are mixed and the hybridization matrix element $V$ controls the mixing strength. In the particle-hole symmetric model that we consider in the following, $t_{ij} = t$ for nearest neighbor sites on the square lattice and zero otherwise and $\epsilon_f = -U/2$. The magnetic field is coupled to the $c$ and $f$ electron spins only. The $g$ factors of the $c$ and $f$ electrons are chosen to be the same, $g_c = g_f = 2$, for simplicity but choosing them differently would not change the qualitative aspects of our conclusions. In the following, the magnetic field is measured in the units of Zeeman energy.

In the non-interacting ($U = 0$) case the ground state of the PAM is a paramagnetic band insulator with the quasi-particle gap $\Delta^0_{qp} = \sqrt{(W/2)^2 + V^2} - W/2 \simeq \frac{V^2}{W}$, where $W$ is the conduction electron bandwidth. In the field, the Zeeman splitting reduces the quasi particle gap. For fields larger than $B_{c1} = \Delta^0_{qp}$, the gap vanishes and the ground state is metallic. In the fields beyond $B_{c2} = \sqrt{(W/2)^2 + V^2} + W/2 \simeq W + 2V^2/W$, all the spins are aligned with the field. The fully polarized ground state consists of two completely filled bands and is a trivial band insulator.

Because of the particle-hole symmetry, the Fermi surfaces of the spin up electrons and the spin down holes in the metallic state at intermediate fields are perfectly nested with respect to $Q = (\pi, \pi)$. The staggered susceptibility in the plane perpendicular to the field diverges logarithmically as $\omega \to 0$. This divergence makes the state unstable under perturbations coupling to the staggered magnetization. In particular, one expects that a staggered magnetization will be induced by any non-zero correlation on the $f$ sites. The ensuing ordered state is a canted antiferromagnet, characterized by both $m_z$ and $m_x$ different from zero.

When $U$ is large enough ($U/V \gg 1$) to suppress charge fluctuations on the $f$ sites, the low-energy physics of PAM is well described by the Kondo lattice model (KLM) [9,16],

$$H_{\text{KLM}} = -t \sum_{\langle i,j\rangle\sigma} c^\dagger_{i\sigma} c_{j\sigma} + J \sum_i \vec{S}^c_i \cdot \vec{S}^f_i - 2B_z \sum_i (S^{z,f}_i + S^{z,c}_i). \quad (2)$$

In the KLM, the charge fluctuations on the $f$ sites are completely suppressed, $f$ electrons are treated as spins and the hybridization is replaced by an antiferromagnetic exchange interaction between conduction electrons and $f$ spins. Formally PAM and KLM can be related by the Schrieffer-Wolff transformation [12,16], yielding $J = 8V^2/U$.

The zero-temperature, zero-field phase diagram of the $2D$ particle-hole symmetric KLM has been well established by various numerical methods [7,8,17]. In the absence of the magnetic field the ground state of the KLM is a paramagnetic insulator at large $J/t$. There is a quantum critical point at $J/t \simeq 1.4$ and for small $J/t$ the ground state is antiferromagnetically ordered.

The large $J/t$ paramagnetic state of the KLM is adiabatically connected to the $U = 0$ state of the PAM. In the particle-hole symmetric case, on finite lattices, this

$$E^{\sigma}_{p,\pm}(k) = \frac{1}{\sqrt{2}}\Big[(B+Um_z)^2 + (Um_x)^2 + 2V^2 + (\epsilon_k - p_\sigma B)^2 \pm \sqrt{((Um_x)^2 + (B+Um_z)^2 - (\epsilon_k - p_\sigma B)^2)^2 + 4V^2[(\epsilon_k - 2p_\sigma B - p_\sigma U m_z)^2 + (Um_x)^2]}\Big]^{1/2} \quad (4)$$

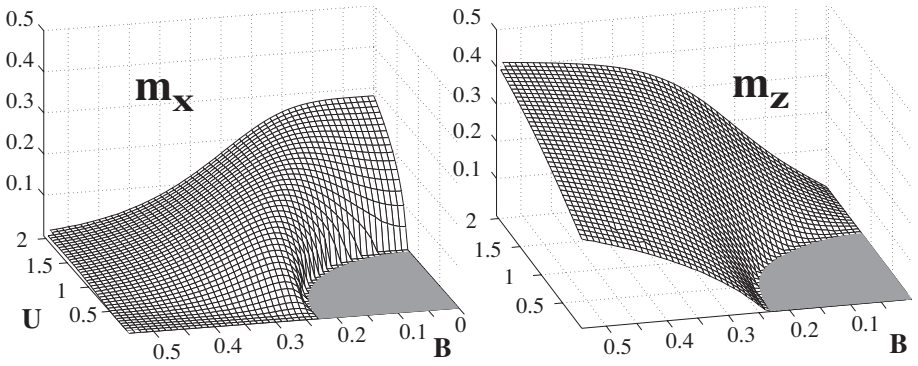


**Fig. 1.** Staggered (left) and parallel magnetizations vs. $B$ and $U$ for $W = 1, V = 1$ obtained by numerically minimizing the mean field equations. The grayed out plateau marks the paramagnetic phase.

is guaranteed by theorems for the ground states of the two models [9].

## 3 Mean field analysis

In this section we investigate the effect of the magnetic field on the small-$U$ PAM. In particular we want to investigate the spin density wave instability of the metallic state induced by the field in the non-interacting model. To this end, we perform the mean field decoupling of the interaction term in equation (1) by assuming the magnetization of the $f$ spins to have a uniform component along the field axis and a staggered component in the plane perpendicular to the field, $\langle \vec{S}^f_i \rangle = \vec{m}_i$ with $\vec{m}_i = \big((-)^i m_x, 0, m_z\big)$. This yields the mean field Hamiltonian (see Appendix A for details of the derivation),

$$H_{MF} = \sum_{k,\sigma}(\epsilon_k - p_\sigma B)c^\dagger_{k\sigma}c_{k\sigma} + \sum_{k,\sigma}(-p_\sigma)(B+Um_z)f^\dagger_{k\sigma}f_{k\sigma} + V\sum_{k,\sigma}\Big(c^\dagger_{k\sigma}f_{k\sigma} + f^\dagger_{k\sigma}c_{k\sigma}\Big) - Um_x\sum_k\Big(f^\dagger_{k+Q\uparrow}f_{k\downarrow} + f^\dagger_{k+Q\downarrow}f_{k\uparrow}\Big) + NU(m_x^2 + m_z^2), \quad (3)$$

with $p_\sigma = 1(\uparrow), -1(\downarrow)$ and $\epsilon_k = -\frac{W}{2}[\cos(k_x) + \cos(k_y)]$. The mean field Hamiltonian is quadratic in fermion operators and is easily diagonalized by a unitary transformation. In the presence of the staggered magnetization, the Brillouin zone is halved and one finds 8 quasi particle bands; the particle bands

*see equation* (4) *above*

and the hole bands related by, $E^{\sigma}_{h,s}(k) = -E^{\bar{\sigma}}_{p,s}(k)$. Note that the $k$ dependence of the quasi-particle bands originates only from the dispersion of the conduction electrons. On a bipartite lattice, with $\epsilon_{k+Q} = -\epsilon_k$, the quasi particle bands satisfy, $E^{\sigma}_{h,s}(\epsilon_k) = -E^{\bar{\sigma}}_{p,\bar{s}}(\epsilon_{k+Q})$.

In the ground state, the particle bands are empty and the hole bands are completely filled. To obtain the ground state energy, the expression

$$E_{gs} = \sum_{s,\sigma}{\sum_k}' E^{\sigma}_{h,s}(k) + \frac{(Um_x)^2 + (Um_z)^2}{U} \quad (5)$$

must be minimized with respect to $m_x$ and $m_z$, yielding the usual mean-field equations,

$$\frac{\partial E_{gs}}{\partial(Um_{x,z})} = 0. \quad (6)$$

The prime on the summation sign in equation (5) indicates that the summation is to be taken over the magnetic Brillouin zone.

### 3.1 Mean field phase diagram

The minimization of the ground state energy for a range of $U$ and $B$ values was performed numerically and the obtained magnetization values are shown in Figure 1. In zero field, the system is paramagnetic at small values of $U$ and antiferromagnetically ordered beyond $U_c \simeq 1.25$ V. The staggered magnetization grows as $(U - U_c)^{1/2}$ close to $U_c$ and tends to the fully saturated value $m_x = 1/2$ as $U \to \infty$.

The magnetic field applied to the system reduces the value of $U$ at which the magnetic instability occurs. The phase boundary can be obtained by solving

$$\frac{2}{U_c(B)} = -\left.\frac{\partial^2 E_0}{\partial(Um_x)^2}\right|_{m_x=0}, \quad (7)$$

where $E_0 = \sum_{s=\pm,\sigma=\uparrow\downarrow}\sum_k E^{\sigma}_{h,s}(k)$. At small fields, $B \ll B_{c1}$, the critical interaction strength falls off as the square

root of the field, $U_c(B) - U_c(0) \propto -\sqrt{B}$, as expected in the mean field approach. At the phase boundary one finds the usual mean field critical exponents for the staggered magnetization, $m_s^x \propto (U - U_c(B))^{1/2}$ and $m_s^x \propto (B - B_c(U))^{1/2}$. After the initial rise, $m_x$ goes through a maximum and falls of exponentially in large fields. On the phase boundary, the parallel susceptibility vanishes (it is zero in the paramagnetic phase, since the spin excitations are gaped). Close to the phase boundary, it behaves like $m_z \propto (B - B_c(U))^{\alpha}$, with $\alpha > 1$.

The right hand side of equation (7) is proportional to the static staggered susceptibility of the $Um_x = 0$ state, $\chi_0^{+-}(Q)$. This can be expressed using the familiar Lindhardt formula which in the case considered here reduces to

$$\chi_0^{+-}(Q) = -\sum_k{}' \left. \frac{f(E^{\downarrow}_{h,-}(k)) - f(E^{\uparrow}_{p,-}(k))}{E^{\downarrow}_{h,-}(k) - E^{\uparrow}_{p,-}(k)} \right|_{Um_x=0}. \quad (8)$$

In small fields, the quasi-particle gap provides a cut-off for the denominator in the sum on the right hand side and $\chi_0^{+-}(Q)$ is finite. When the field closes the gap, the denominator vanishes along the Fermi surface (Fermi lines), determined by the equation,

$$\epsilon_k = \pm\epsilon_0 = \pm\frac{V^2 - BUm_z - B^2}{B + Um_z}. \quad (9)$$

Consequently, the staggered susceptibility diverges logarithmically in the field $B > \Delta^0_{qp}$ and there is no finite $U_c$. The system is ordered for any finite interaction strength. The divergence of $\chi_0^{+-}(Q)$ is a direct consequence of the perfect nesting, $E^{\downarrow}_{h,-}(k) = -E^{\uparrow}_{p,-}(k)$, and is found at all fields, if the conduction electron hopping is constrained to a bipartite lattice and the system is half filled[1].

The behavior of the staggered magnetization at small $U$ can be found by solving the mean field equations to leading logarithmic order in $Um_x$. The details of the calculation are described in Appendix A. The resulting expression for the magnetization is

$$m_x \propto \exp\left[-\frac{(B + Um_z)^4 + V^2(B + Um_z)^2}{V^4\rho_0 U}\right], \quad (10)$$

where $\rho_0$ is taken to be the density of states on the $m_x = 0$ Fermi surface. It is interesting to note that the expression (10) is valid for the large field region and for the large $U$ region with $B \gg 8V^2/U$.

### 3.2 Quasi-particle spectrum

The field dependence of the quasi-particle gap for a fixed value of the interaction is shown in Figure 2. In the paramagnetic phase, the gap decreases linearly with the field. In the ordered phase, the quasi-particle gap is proportional to the staggered moment and follows the same exponential dependence for large fields. It is important to realize that the quasi-particle gap always remains finite, so that the system is insulating.

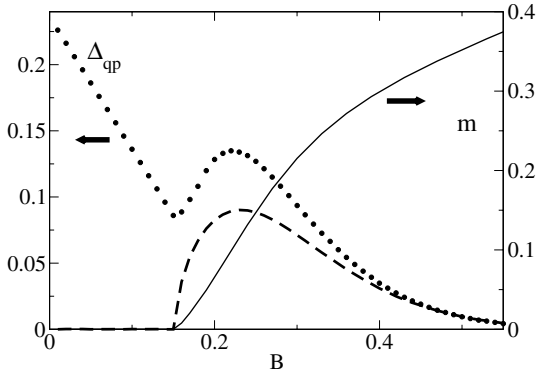


**Fig. 2.** Quasi-particle gap (dots), staggered magnetization (dashed line) and total ($f + c$) parallel magnetization (thin solid line) vs. magnetic field for $W = 4$, $V = 1$, $U = 1$. In the paramagnetic phase the gap decreases linearly with field. At large fields the gap follows the staggered magnetization.

The spectral functions for the electrons in the mean field model show infinitely sharp peaks at the quasi-particle band energies. The poles of the $\sigma =\uparrow$ electron spectral function in the ordered phase at various values of the field and interaction strengths are shown in Figure 3. The width of the lines in the figure indicate the weights in the corresponding poles. Note that the gap at the Fermi surface is always finite, even though the exponentially small scale is not immediately apparent in the plots. The contour plots show the quasi-particle gap size in the Brillouin zone. The gap minima are indicated by the dashed lines in the contour plots. The location of the gap minima indicates also the position of the Fermi surfaces of the $m_x = 0$, metallic state.

It is interesting to observe the change in the character of the quasi-particles at the gap minima as the field and the interaction strength are varied. At small $U$ and $B \simeq \Delta^0_{qp}$, the low-energy quasi-particles are "heavy" and the minimum of the gap lies near the zone center. As the field is increased, the minimum moves towards the zone diagonal and the quasi-particles become more and more $c$ like.

When the gap minimum reaches the zone diagonal, the magnetization of the system along the field direction is exactly one half of the fully saturated value. The field strength at which this happens, $B_{1/2}$, depends on the interaction strength and can be obtained by setting $\epsilon_0 = 0$ with the limiting behavior:

$$B_{1/2} \to \begin{cases} V, & U \to 0 \\ \dfrac{2V^2}{U}, & U \to \infty. \end{cases} \quad (11)$$

In the large $U$ limit, $B_{1/2}$ sets the energy scale at which the $f$ electrons align with the field.

[1] Note that, the shape of the Fermi lines is determined only by the conduction electron dispersion and the surface they enclose by the half-filling condition. Therefore, the perfect nesting in the half-filled system can not be removed by changing the ratio of $g$ factors or by changing $\epsilon_f$.

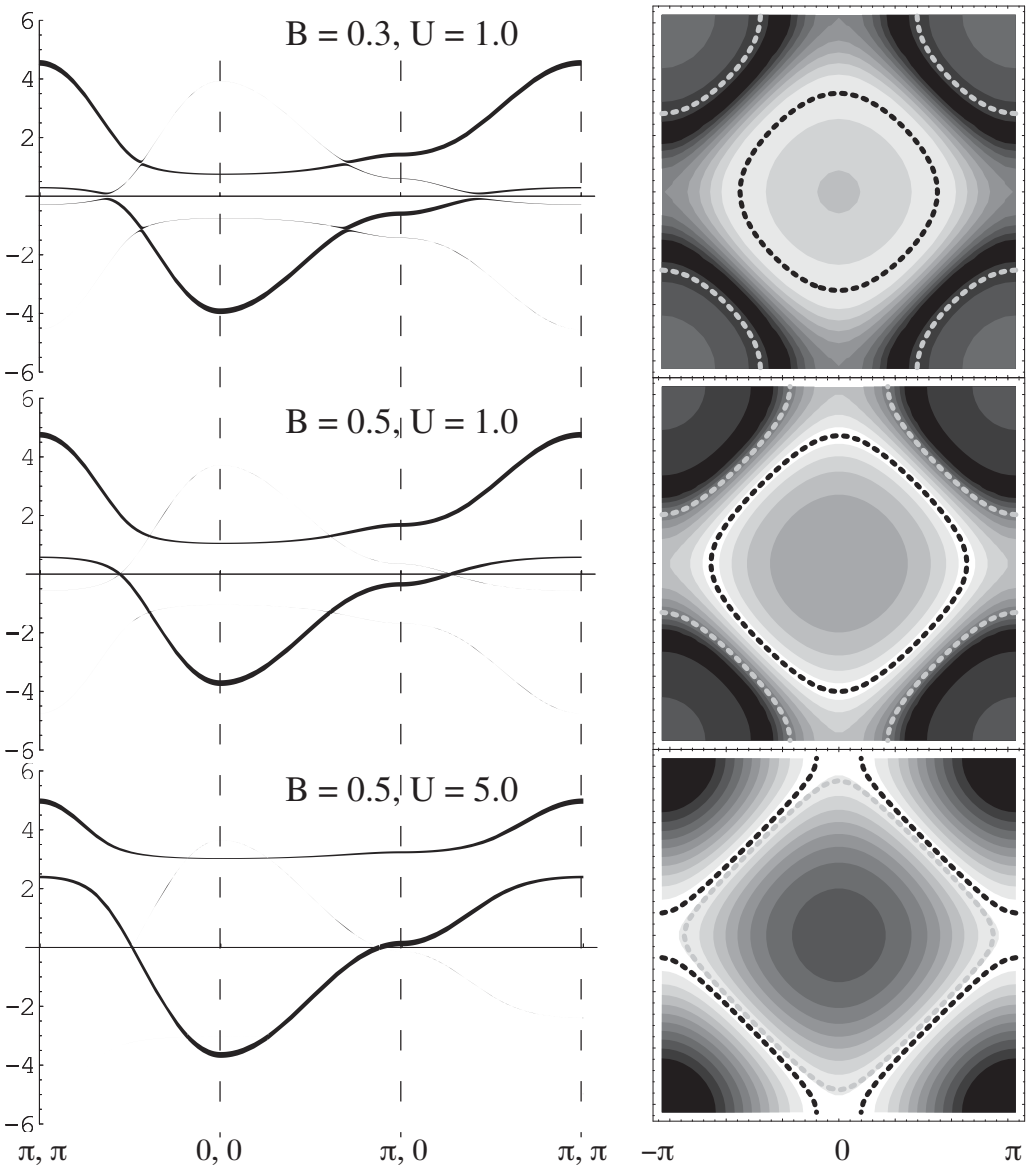


**Fig. 3.** Poles of the $\sigma =\downarrow$ conduction electron spectral functions along the high symmetry lines of the Brillouin zone for field and interaction strengths indicated in the plots. The width of the lines indicates the weight in the pole. The plots on the right show the contours of constant quasi-particle gap magnitude with dashed lines indicating the position of the Fermi surfaces of the $m_x = 0$ state.

## 4 Large B limit of the Kondo model

For large values of $U$, in the fields $B > B_{1/2}$, the $f$ electrons are almost completely aligned with the field. At the mean field level, the poles of the spectral function corresponding to the charge fluctuations on the $f$ sites move towards $\pm(B + Um_z)$, i.e. far from the Fermi level. In the large-$N$ mean field theory this eventually results in the complete decoupling of the $f$ electrons from the $c$ band and the decoupled metallic state obtains [11].

In the particle hole symmetric case, the Fermi surfaces of the metallic state are perfectly nested. The perfect nesting makes the metallic state unstable at all fields in the small $U$ limit of the PAM. We will now demonstrate that also in the limit of large Coulomb interaction, i.e. for the KLM, the same instability arises.

### 4.1 Effective Hamiltonian approach

We consider the KLM Hamiltonian in the large magnetic field $B \gg J$. In the magnetic field, the $J = 0$ ground state of the KLM is non degenerate and is given by $|\psi\rangle = \prod_{k<k_{F\uparrow}} c^\dagger_{k\uparrow} \prod_{k<k_{F\downarrow}} c^\dagger_{k\downarrow} \prod_i f^\dagger_{i\uparrow}|\rangle$. Flipping the $f$ spin is an excitation with a gap given by the Zeeman energy. A canonical transformation approach can be used to generate an expansion in $(J/B)$ around the $J = 0$ ground state. The effective Hamiltonian governing the low energy

dynamics of the system is given by (the details of the derivation in Appendix B),

$$\tilde{H} = \sum_{k\sigma}(\epsilon_k - p_\sigma \tilde{B})c^\dagger_{k\sigma}c_{k\sigma} + \tilde{U}\sum_i n_{i\uparrow}n_{i\downarrow} \qquad (12)$$

where $\tilde{U} = \frac{J^2}{8B}$, $\epsilon_k$ is the dispersion of the original conduction electron band and $\tilde{B} = (B - J/4 - \tilde{U}/2)$ is the effective magnetic field. In this effective model, the spin flip interaction between the conduction band and the fully polarized $f$-spin background of the KLM, has been replaced by a contact interaction between the $c$ electrons and the $f$ spins have decoupled from the dynamics.

If the conduction electron band is particle hole symmetric, so that $\epsilon_{k+Q} = -\epsilon_k$, the spin up hole and the spin down electron Fermi surfaces of the effective model are perfectly nested. Any non zero $\tilde{U}$ therefore induces magnetic ordering in the plane perpendicular to the applied field. A mean-field decoupling, with $\langle \vec{s}_i \rangle = ((-)^i m_x, 0, m_z)$, analogous to the one performed in Section 3, yields the quasi particle bands

$$E_{\sigma,\pm}(k) = \pm\sqrt{(\epsilon_k - p_\sigma(\tilde{B} + \tilde{U}m_z))^2 + (Um_x)^2} \qquad (13)$$

and the mean-field equation determining $m_x$,

$$\frac{2}{\tilde{U}} = \int_{-W}^{0} \rho(\epsilon)d\epsilon \left[\frac{1}{E_{\uparrow,+}(\epsilon)} + \frac{1}{E_{\downarrow,+}(\epsilon)}\right]. \qquad (14)$$

In high magnetic fields, the up and down spin Fermi surfaces are well approximated by circles of radii $W - \tilde{B}$ centered at $(\pi, \pi)$ and $(0, 0)$, respectively. We therefore can set $\rho(\epsilon) = \rho_0 = v_F^{-1}$ to obtain

$$\tilde{U}m_x \propto 2(W - \tilde{B} - \tilde{U}m_z)\exp\left(-\frac{1}{\rho_0\tilde{U}}\right). \qquad (15)$$

The staggered magnetization and the quasi-particle gap are finite for any finite $\tilde{U}$, as long as $\tilde{B} + \tilde{U}m_z < W$. It is easy to see that, $\tilde{B} + \tilde{U}m_z = W$ is just the condition for system to fully polarize. This means that the staggered magnetization vanishes only in the completely polarized system. The completely polarized phase is a trivial insulator. The metallic state is, therefore, never obtained in the particle-hole symmetric case and is a bad starting point for the perturbation expansion.

### 4.2 Classical spins mean field

We have seen that a large magnetic field suppresses both charge and spin fluctuations on the $f$ sites. The physics of the high-field phase will, therefore, be well described by the KLM in which the $f$ spins are replaced by an array of statically arranged classical spins. Let the spin configuration be

$$\vec{S}_i = \frac{1}{2}\begin{pmatrix} \sin\theta\cos Qr_i \\ -\sin\theta\sin Qr_i \\ \cos\theta \end{pmatrix}. \qquad (16)$$

With $Q = (\pi, \pi)$, this corresponds to the same choice of $f$ magnetization as in Section 3, with $1/2\sin\theta = m_x$ and $1/2\cos\theta = m_z$, so that the system is fully polarized for $\theta = 0$. The problem is now reduced to one of the non-interacting conduction electrons in an external magnetic field, described by the Hamiltonian,

$$H = \sum_{k,\sigma}\left(\epsilon_k - p_\sigma\tilde{B}\right)c^\dagger_{k\sigma}c_{k\sigma} - NB\cos\theta + \frac{J\sin\theta}{4}\sum_k\left(c^\dagger_{k-Q\uparrow}c_{k\downarrow} + c^\dagger_{k+Q\downarrow}c_{k\uparrow}\right), \qquad (17)$$

with $\tilde{B} = B - J/4\cos\theta$. This is easily diagonalized to find the quasi-particle bands ($k$ in the magnetic Brillouin zone),

$$E_{\sigma,\pm}(k) = \pm\sqrt{(\epsilon_k - p_\sigma\tilde{B})^2 + (J/4)^2\sin^2\theta}. \qquad (18)$$

In the ground state the "−" bands are completely filled. Minimizing the ground state energy and assuming the same circular Fermi surface approximation as in the previous subsection, the mean field equation determining the angle $\theta$ is obtained as,

$$B\tan\theta = \rho_0\int_{-W}^{0}\sum_\sigma\left[\left(\frac{J}{4}\right)^2\sin\theta - p_\sigma(\epsilon - p_\sigma\tilde{B})\frac{J}{4}\tan\theta\right]\frac{1}{E_{\sigma,+}}. \qquad (19)$$

For $\sin\theta \ll 1$ ($f$ moments almost aligned with the field) we obtain,

$$Jm_x \propto \sqrt{(W - \tilde{B})(W + \tilde{B})}\exp\left[-\frac{8B}{\rho_0 J^2} + \frac{4\rho_0 B + 8}{\rho_0 J}\right]. \qquad (20)$$

The staggered magnetization vanishes only when $\tilde{B} = W$. It is easy to see that this is exactly the condition for the system to fully polarize. The full polarization field is equal to $W - J/4$ and agrees with the one obtained using the effective Hamiltonian. The dominant, small $J$ exponential dependence of the staggered magnetization $m_x \propto \exp[-8B/(\rho_0 J^2)]$ also agrees with the one obtained in the previous section. The subleading $1/(\rho_0 J)$ correction to the exponent arises because the Zeeman energy of the $f$ electrons has now been taken into account. As the quasi-particle gap is proportional to the staggered magnetization, the system stays insulating at all fields.

## 5 Quantum Monte Carlo

In this section we present QMC simulations of the Kondo lattice model in the magnetic field. As in the zero field case, the sign problem may be avoided only for particle-hole symmetric conduction bands. To compare with the mean-field results we adopt a projective approach in which

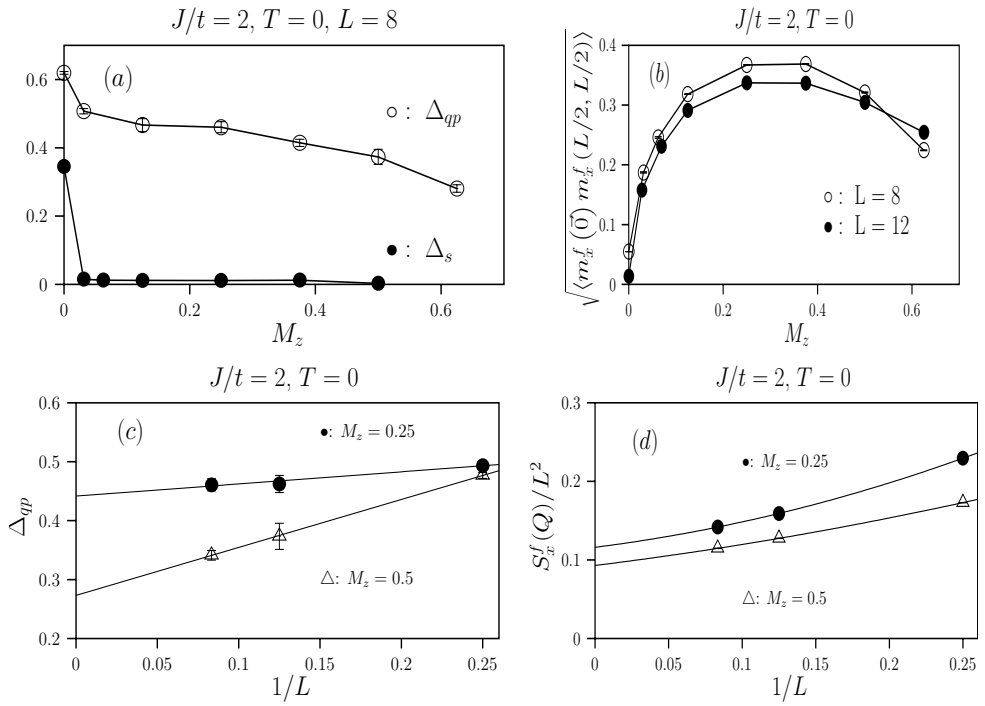


**Fig. 4.** (a) Quasi-particle and spin gaps as a function of the magnetization; (b) $x$-component of the $f$-spin-spin correlations at the largest distance, ($L/2$, $L/2$), on the $L \times L$ lattice. The Fourier transform of this quantity, $\sum_{\vec{r}} e^{i\vec{q}\cdot\vec{r}} \langle m_x^f(\vec{0}) m_x^f(\vec{r})\rangle$, is peaked at the antiferromagnetic wave vector, $\vec{Q} = (\pi, \pi)$. (c) Size scaling of the quasi-particle gap at $M_z = 0.25, 0.5$. The data is consistent with a finite value of $\Delta_{qp}$ in the thermodynamic limit. (d) Size scaling of $S_x^f(\vec{Q} = (\pi, \pi)) = \sum_{\vec{r}} e^{i\vec{Q}\cdot\vec{r}} \langle m_x^f(\vec{r}) m_x^f(\vec{0})\rangle$ for $M_z = 0.5, 0.25$ As apparent, the data is consistent with $S_x^f(\vec{Q}) \sim L^2$ thus signaling the presence of long-range antiferromagnetic order perpendicular to the applied field.

the ground state, $|\Psi_0\rangle$, is filtered out from a trial wave function, $|\Psi_T\rangle$, satisfying $\langle\Psi_0|\Psi_T\rangle \neq 0$. In this algorithm, the ground state expectation value of an observable $O$ is estimated via:

$$\frac{\langle\Psi_0|O|\Psi_0\rangle}{\langle\Psi_0|\Psi_0\rangle} = \lim_{\Theta\to\infty} \frac{\langle\Psi_T|e^{-\Theta H/2} O e^{-\Theta H/2}|\Psi_T\rangle}{\langle\Psi_T|e^{-\Theta H}|\Psi_T\rangle}. \qquad (21)$$

In the QMC, we evaluate the right hand side of the above expression at finite values of $\Theta$ and then extrapolate to infinite values. The details of the algorithm — in particular the sign free formulation — has been described extensively in reference [8]. Since we are working in the canonical ensemble, the total magnetization

$$M_z = \frac{N_c^{\uparrow} + N_f^{\uparrow} - N_c^{\downarrow} - N_f^{\downarrow}}{N_u} \qquad (22)$$

with $N_u$ the number of unit cells, is fixed during the simulations.

By measuring time displaced correlation functions, we can extract quasi-particles as well as spin gaps. Consider

$$\langle\Psi_0|S^-(-q,\tau)S^+(q,0)|\Psi_0\rangle = \sum_n |\langle n|S^+(q)|\Psi_0\rangle|^2 e^{-\tau(E_n(q,N,S_z+1)-E_0(N,S_z))} \qquad (23)$$

where $E_n(q, N, S_z)$ are eigenstates of $H$ with momentum $\vec{q}$, particle number $N$ and total $z$-component of spin $S_z$. From the large $\tau$ behavior of the above correlation functions, we can extract the energy difference $E_0(q, N, S_z+1) - E_0(N, S_z)$ from which we can determine the spin gap:

$$\Delta_{sp}(\vec{q}) = E_0(\vec{q}, N, S_z + 1) - E_0(N, S_z) - h \qquad (24)$$

where $h = [E_0(N, S_z + 1) - E_0(N, S_z - 1)]/2$. In the same manner, we compute the quasi-particle gap from the single-particle imaginary time displaced Green function

$$\Delta_{qp}(\vec{k}) = E_0(\vec{k}, N + 1, S_z) - E_0(N, S_z) - \mu \qquad (25)$$

with chemical potential: $\mu = [E_0(N + 1, S_z) - E_0(N - 1, S_z)]/2$. In Figure 4 we plot the gaps as a function of total magnetization at $J/t = 2.0$.

In the zero field case, the Kondo insulating state with finite quasi-particle and spin gaps is realized. At finite magnetizations and according to the mean-field approach, we expect a canted antiferromagnetic state and hence no spin gap. Figure 4 confirms this point of view: the spin gap drops to zero at all finite values of the magnetization within the accuracy of the numerical simulation and the equal time spin-spin correlations in the plane perpendicular to the magnetic field show long range antiferromagnetic order. In the mean-field approach, magnetism stems from a Fermi surface instability and due to perfect nesting opens a gap on all the Fermi line. The QMC results of Figure 4 are consistent with this prediction,

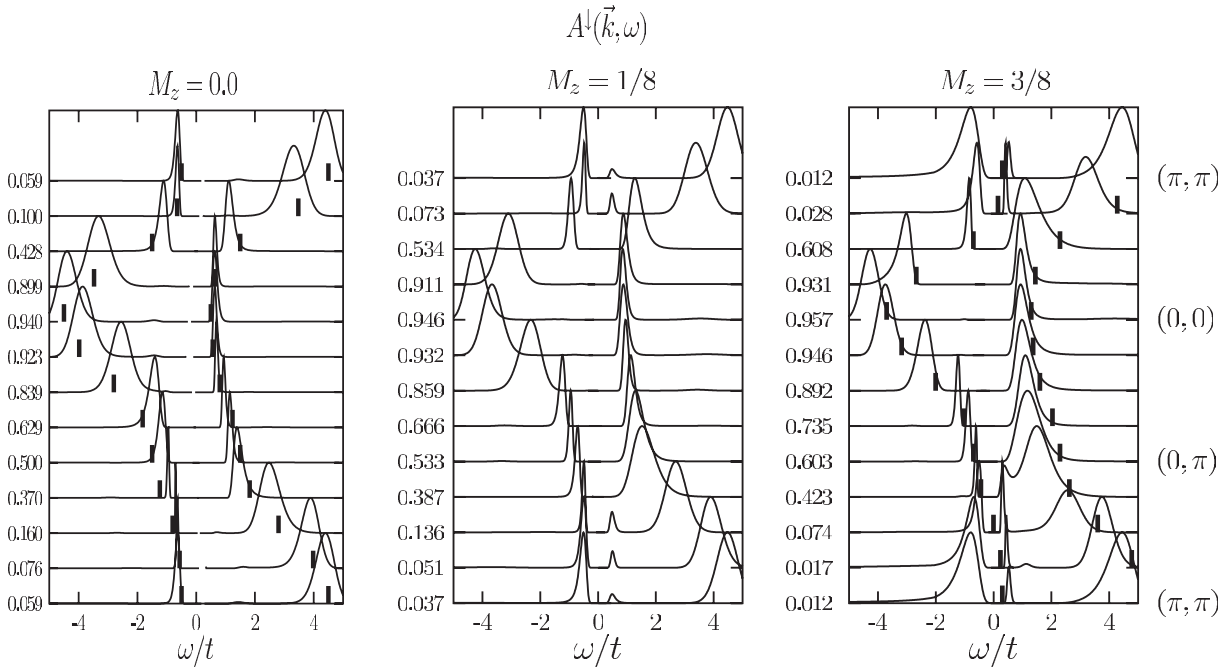


**Fig. 5.** Single particle spectral function in the down-spin sector as a function of magnetization as obtained from analytical continuation of the QMC results with the Maximum Entropy method. The solid vertical lines correspond to the pole position of hybridized bands (see text). On the left hand side of each figure we have listed the single particle occupation number $n_{\vec{k},\downarrow}$ from which one can determine the weight under the spectral function (see Eq. (26)).

since, as apparent, the quasi-particle gap survives at finite magnetizations.

To further compare the mean-field approach to the QMC we have used the Maximum Entropy method to obtain the single particle spectral function $A(\vec{k},\omega)$. At zero field in the Kondo insulating phases, the dominant features of the spectral function are well described by hybridized bands (solid vertical lines in Fig. 5a). From the single particle occupation number $n_{\vec{k},\sigma} = \langle c^{\dagger}_{\vec{k},\sigma} c_{\vec{k},\sigma} \rangle$ listed on the left hand side of Figures 5a–5c we can extract the total weight under the "photoemission" ($\omega < 0$) and the "inverse photoemission" ($\omega < 0$) spectra since

$$\int_{-\infty}^{0} \mathrm{d}\omega A^{\sigma}(\vec{k},\omega) = \pi n_{\vec{k},\sigma} \quad \int_{0}^{\infty} \mathrm{d}\omega A^{\sigma}(\vec{k},\omega) = \pi(1 - n_{\vec{k},\sigma}). \tag{26}$$

In particular, one sees that the photoemission (inverse photo-emission) spectrum in the vicinity of $\vec{k} = (\pi,\pi)$ ($\vec{k} = (0,0)$) has a small weight. Those heavy bands stem from the Kondo screening.

In the mean field approach, the effect of a magnetic field is to shift the spin down band up in energy until it ultimately crosses the Fermi surface, thus generating a metallic state. This metallic state is however unstable due to the underlying particle-hole symmetry. In Figure 5c we compare the finite field results with a rigid shift of the hybridized bands. The data are compatible with the interpretation that the down spin band has indeed crossed the Fermi surface but that at the crossing point the magnetic instability opens a gap. Furthermore on the photo-emission side around the $(\pi,\pi)$ point we see a very weak feature which we can identify as a shadow of the up band which has dropped below the Fermi energy in the vicinity of the $\vec{k} = (0,0)$ point.

Breaking of the spin symmetry by the magnetic field suppresses Kondo screening. We hence expect the weight of the features in the spectral function stemming from Kondo screening to be suppressed as a function of growing magnetization. For example, consider the inverse photoemission at $\vec{k} = (0,0)$ in Figure 5. As apparent the weight of this feature is reduced as a function of growing values of $M_z$ and will vanish when the $f$-spins become fully polarized. In our simulations, the $f$-spins are never completely aligned with the field as long as the system is not completely polarized, i.e. as long as $N_c^{\uparrow} + N_f^{\uparrow} < N_u$. This supports the conclusion that the metallic state is never induced by the field.

## 6 Conclusion

We studied the magnetic field induced quantum phase transition in the 2D particle-hole symmetric Kondo insulators using: (i) a mean field approximation appropriate in the small $U$ limit of the periodic Anderson model, (ii) two mean field approximations appropriate in the large field limit of the Kondo lattice model and (iii) a quantum Monte Carlo simulation of the particle-hole symmetric 2D Kondo lattice model in the field.

We find a magnetic field induced quantum phase transition from a paramagnetic insulator into a canted

antiferromagnetic insulator ground state. In the particle-hole symmetric case we studied, the antiferromagnetism can be understood as a spin density wave type instability of the perfectly nested quasi-particle Fermi surfaces that would arise in the field in the absence of interactions. Because of the perfect nesting, any finite interaction is a relevant perturbation and results in a finite quasi-particle gap. Consequently, the ground state of the interacting system remains insulating in all fields.

We conclude that the recently proposed insulator to metal transition induced by the field [11] is likely to be an artifact of the large-$N$ approximation to the Kondo lattice model in the particle-hole symmetric case. If, however, the particle-hole symmetry is violated a field-induced metal-insulator transition is possible in certain parameter ranges.

We find that the qualitative features of the phase diagram as well as of the quasi-particle excitations are well described by a simple mean field approximation to the periodic Anderson model. The magnetic field explicitly breaks the spin rotation symmetry and suppresses the charge fluctuations on $f$ electrons, essentially by fully polarizing the $f$ band.

The band structure of the Kondo insulators is non-trivial and deviations from particle-hole symmetry are to be expected in the real materials. In the absence of perfect nesting there would be a critical value of the field, controlled essentially by the nesting mismatch, at which the gap will close on some parts of the Fermi surface. Therefore one expects to eventually find a metallic state induced by the field. Finally we would like to mention that the conclusions we draw here are valid also for the three-dimensional systems, where the same kind of nesting features would appear for perfect particle-hole symmetry.

We would like to thank P.A. Lee, T.M. Rice, K.D.S. Beach and S. Wehrli for helpful discussions. This work was financially supported by the Swiss Nationalfonds and, in particular, by the NCCR program MaNEP. F.F. Assaad thanks the DFG for financial support under the grant number of AS 120/1-1 as well as the hospitality of the ITP of the ETHZ where part of this work was carried out. The calculations were performed on the Cray-T3E as well as on the IBM-p690 in Jülich. We thank this institution for generous allocation of CPU time.

## Appendix A: Mean field decoupling of the Hubbard term in the canted anti-ferromagnetic phase

We want to decouple the interaction term in the PAM, in the presence of a canted staggered magnetization. To this end, we select the spin quantization axis at each site to point in the direction of the local magnetization, $\vec{m}_i$. Using the operator identity $f^\dagger_{i\uparrow_i} f_{i\uparrow_i} f^\dagger_{i\downarrow_i} f_{i\downarrow_i} = 1/4(f^\dagger_{i\uparrow_i} f_{i\uparrow_i} + f^\dagger_{i\downarrow_i} f_{i\downarrow_i})^2 - 1/4(f^\dagger_{i\uparrow_i} f_{i\uparrow_i} - f^\dagger_{i\downarrow_i} f_{i\downarrow_i})^2$, where $\uparrow_i$ ($\downarrow_i$) denotes the spin with respect to the local quantization axis, the interaction term can be decoupled as

$$\begin{aligned} U \sum_i f^\dagger_{i\uparrow_i} f_{i\uparrow_i} f^\dagger_{i\downarrow_i} f_{i\downarrow_i} = {} & \frac{Un_f}{2} \sum_i (f^\dagger_{i\uparrow_i} f_{i\uparrow_i} + f^\dagger_{i\downarrow_i} f_{i\downarrow_i}) \\ & - N\frac{Un_f^2}{4} - U \sum_i |\vec{m}_i| (f^\dagger_{i\uparrow_i} f_{i\uparrow_i} \\ & - f^\dagger_{i\downarrow_i} f_{i\downarrow_i}) + U|\vec{M}|^2 \\ & + \text{Fluct.} \end{aligned} \tag{A.1}$$

where $n_f = \langle f^\dagger_{i\uparrow} f_{i\uparrow} + f^\dagger_{i\downarrow} f_{i\downarrow} \rangle$ is the average occupancy of the $f$ site and "Fluct." denotes the terms neglected in the mean-field approximation. After the decoupling, a spin axis rotation to a common quantization axis (given by the direction of the external field) is performed using $\hat{R} = \exp\left(\sum_i -i/2\vec{\theta}_i \cdot \vec{S}^f_i\right)$ with $\vec{\theta}_i$ being the vector pointing along $\vec{B} \times \vec{m}_i$ and of magnitude equal to the angle between $\vec{B}$ and $\vec{m}_i$. Since,

$$|\vec{m}_i| \hat{R} \tfrac{1}{2} (f^\dagger_{i\uparrow_i} f_{i\uparrow_i} - f^\dagger_{i\downarrow_i} f_{i\downarrow_i}) \hat{R}^\dagger = \vec{m} \cdot \vec{S}^f_i, \tag{A.2}$$

this yields the mean field Hamiltonian, equation (3) of Section 3.

To obtain the behavior of the staggered magnetization in fields $B > \Delta^0_{qp}$ and at small $U$ we need to solve the mean field equations (6), in the limit when $Um_x \to 0$. As the only $k$ dependence of the quasi-particle bands comes through the $k$ dependence of the conduction electron energy, the summations over $k$ are readily transformed into integrals over the conduction electron energy, thus yielding ($\rho(\epsilon)$ is the conduction electron DOS),

$$\frac{\partial}{\partial(Um_x)} \left[ \int_{-W}^{0} \rho(\epsilon) d\epsilon (E^\uparrow_{h,\pm}(\epsilon) + E^\downarrow_{h,\pm}(\epsilon)) \right] + 2\frac{Um_x}{U} = 0. \tag{A.3}$$

For $Um_x \to 0$, the dominant contribution to the integral comes from the band crossing the Fermi surface at $\epsilon_0$ (given by Eq. (9)). For $\Delta^0_{qp} < B < V$, this is $E^\downarrow_{h,+}$. For small $U$ and close to $\epsilon_0$ we can write,

$$E^\downarrow_{h,+}(\epsilon) = \sqrt{\alpha^2 (Um_x)^2 + \beta^2 (\epsilon - \epsilon_0)^2}, \tag{A.4}$$

with

$$\alpha = \frac{V^2}{(B + Um_z)^2 + V^2} \tag{A.5}$$

$$\beta = \frac{(B + Um_z)^2}{(B + Um_z)^2 + V^2}. \tag{A.6}$$

The logarithmically divergent part of the mean field equation can now be written as (neglecting the non-divergent contributions),

$$\frac{1}{U} = \frac{\alpha^2}{\beta} \int_0^{\epsilon_c} \frac{d\epsilon' \rho(\epsilon_0 + \epsilon')}{\sqrt{\left(\frac{\alpha U m_x}{\beta}\right)^2 + \epsilon'^2}}, \tag{A.7}$$

where we have introduced a cutoff $\epsilon_c$ which does not influence the exponential dependence. Equation (10) in the text now follows by elementary integration.

## Appendix B: Effective Hamiltonian in the large field

The ground state of the $J = 0$ KLM in the magnetic field is non-degenerate. All the $f$ spins are polarized in the direction of the field. The $f$ spin flip is an excitation with an energy gap of the size of the Zeeman energy. Let $P_n$ denote the portion of the Hilbert space with $n$ localized spins pointing opposite to the magnetic field and let $\mathcal{P}_n$ be the corresponding projector. In large magnetic fields, $B \gg J$, one expects the ground state and the low lying excitations to lie dominantly in $P_0$ and have only small components in the $P_n$, with $n > 0$, subspaces. We split the $H_{\rm KLM}$ into a $P_n$ diagonal part

$$H_0 = \sum_{k\sigma}(\epsilon_{k\sigma} - p_\sigma B)c^\dagger_{k\sigma}c_{k\sigma} - 2B\sum_\sigma p_\sigma S^z_i + \frac{J}{2}\sum_i S^z_i\left(c^\dagger_{i\uparrow}c_{i\uparrow} - c^\dagger_{i\downarrow}c_{i\downarrow}\right) \quad \text{(B.1)}$$

and the spin flip part

$$V = \frac{J}{2}\sum_i \left(c^\dagger_{i\uparrow}c_{i\downarrow}S^-_i + c^\dagger_{i\downarrow}c_{i\uparrow}S^+_i\right). \quad \text{(B.2)}$$

Let $S$ be a Hermitian operator, such that

$$[H_0, S] = -V. \quad \text{(B.3)}$$

The effective Hamiltonian, obtained by applying the canonical transformation

$$\tilde{H} = e^{-S}H_{\rm KLM}e^S \quad \text{(B.4)}$$

has no matrix elements between the states in $P_0$ and $P_{n>0}$ of order less then $\mathcal{O}(J(J/B)^2)$. We can therefore obtain the low-energy dynamics of the original problem correctly to order $J^2/B$) by considering only the $P_0$ part of the Hilbert space and the Hamiltonian,

$$\tilde{H}^{P_0} = \mathcal{P}_0 e^S H_{\rm KLM}e^{-S}P_0. \quad \text{(B.5)}$$

By expanding and rearranging the exponentials one obtains

$$\tilde{H}^{P_0} = \mathcal{P}_0\left(H_0 + \frac{1}{2}[V,S] + \cdots\right)\mathcal{P}_0. \quad \text{(B.6)}$$

Using equation (B.3) it is easy to obtain the matrix elements of $S$ between the eigenstates of $H_0$ from which the operator form easily follows,

$$S = \frac{J}{4B}\frac{1}{\sqrt{N}}\sum_{kq}\left(S^+_q c^\dagger_{k-q\downarrow}c_{k\uparrow} - S^-_q c^\dagger_{k-q\uparrow}c_{k\downarrow}\right), \quad \text{(B.7)}$$

thus yielding,

$$[V,S] = \frac{J^2}{4B}\frac{1}{N}\sum_{qkk'}\left[S^-_q c^\dagger_{k\uparrow}c_{k-q\downarrow}, S^+_q c^\dagger_{k'\downarrow}c_{k'-q\uparrow}\right]. \quad \text{(B.8)}$$

Evaluating the commutator and projecting on the $P_0$ subspace, yields

$$\mathcal{P}_0[V,S]\mathcal{P}_0 = -\frac{J^2}{4B}\frac{1}{N}\sum_{kk'q} c^\dagger_{k'\downarrow}c_{k'-q\uparrow}c^\dagger_{k\uparrow}c_{k-q\downarrow}. \quad \text{(B.9)}$$

Substituting into equation (B.6) and neglecting the terms corresponding to the dots, which are of order $\mathcal{O}(J^3/B^2)$ one obtains the effective Hamiltonian,

$$\tilde{H} = H_0 + \frac{J^2}{8B}\sum_i s^z_i + \frac{J^2}{8B}\sum_i n_{i\uparrow}n_{i\downarrow} - \frac{J^2N}{16B}. \quad \text{(B.10)}$$

The last term in the above equation is a constant and can be dropped, the $s^z_i$ term is the contribution to the effective uniform magnetic field. This completes the derivation of the effective model described in Section 4.

### *Note added in proof*

In the version of reference [11] published since the submission of this article, the authors have withdrawn the claims of the observation of the metallic state induced by the field. We are pleased that the results of our investigations now seem to be in accord.

## References


1. P.S. Riseborough, Adv. Phys. **49**, 257 (2000)
2. K. Sugiyama, F. Iga, M. Kasaya, T. Kasuya, M. Date, J. Phys. Soc. Jpn **57**, 3946 (1988)
3. J.C. Cooley, C.H. Mielke, W.L. Hults, J.D. Goettee, M.M. Honold, R.M. Modler, A. Lacerda, D.G. Rickel, J.L. Smith, J. Supercond. **12**, 171 (1999)
4. M. Jaime, R. Movshovich, G.R. Stewart, W.P. Beyermann, M.G. Berisson, M.F. Hundley, P.C. Canfield, J.L. Sarrao, Nature **405**, 160 (2000)
5. N.A. de Olivera, J. Phys. Chem. Solids **64**, 1173 (2003)
6. N.A. de Olivera, M. V. Tovar Costa, A. Troper, Gloria M. Japiassu, and M.A. Continentino, Phys. Rev. B **60**, 1444 (1999)
7. Z.P. Shi, R.R.P. Singh, M.P. Gelfand, Z. Wang, Phys. Rev. B **51**, 15630 (1995)
8. S. Capponi, F.F. Assaad, Phys. Rev. B **63**, 155114 (2000)
9. H. Tsunetsugu, M. Sigrist, K. Ueda, Rev. Mod. Phys. **69**, 809 (1997)
10. H.M. Carruzzo, C.C. Yu, Phys. Rev. B **51**, 10301 (1995)
11. K.S.D. Beach, P.A. Lee, P. Monthoux, Phys. Rev. Lett. **92**, 026401 (2004)
12. J.R. Schrieffer, P.A.Wolff, Phys. Rev. **149**, 491 (1966)
13. V. Dorin, P. Schlottmann, Phys. Rev. B **46**, 10800 (1992)
14. R. Doradzinski, J. Spalek, Phys. Rev. B **58**, 3293 (1998)
15. P.S. Riseborough, Phys. Rev. B **45**, 13984 (1992)
16. P. Sinjukow, W. Nolting, Phys. Rev. B **65**, 212303 (2002)
17. W.H. Zheng, J. Oitmaa, Phys. Rev. B **67**, 214406 (2003)